カタログ

Supplemental Figure 1

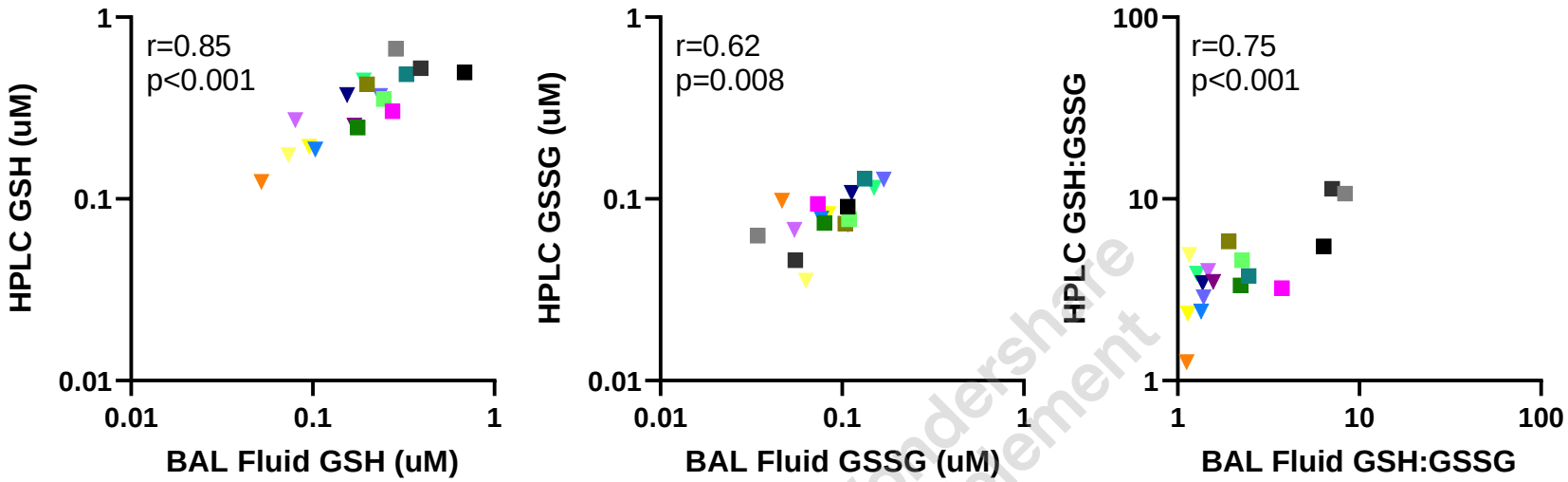

Fig. 1. GSH and GSSG levels and GSH:GSSG measured by enzymatic method correlated strongly with high-performance liquid chromatography (HPLC) measurements (n=17).

Supplemental Figure 2.

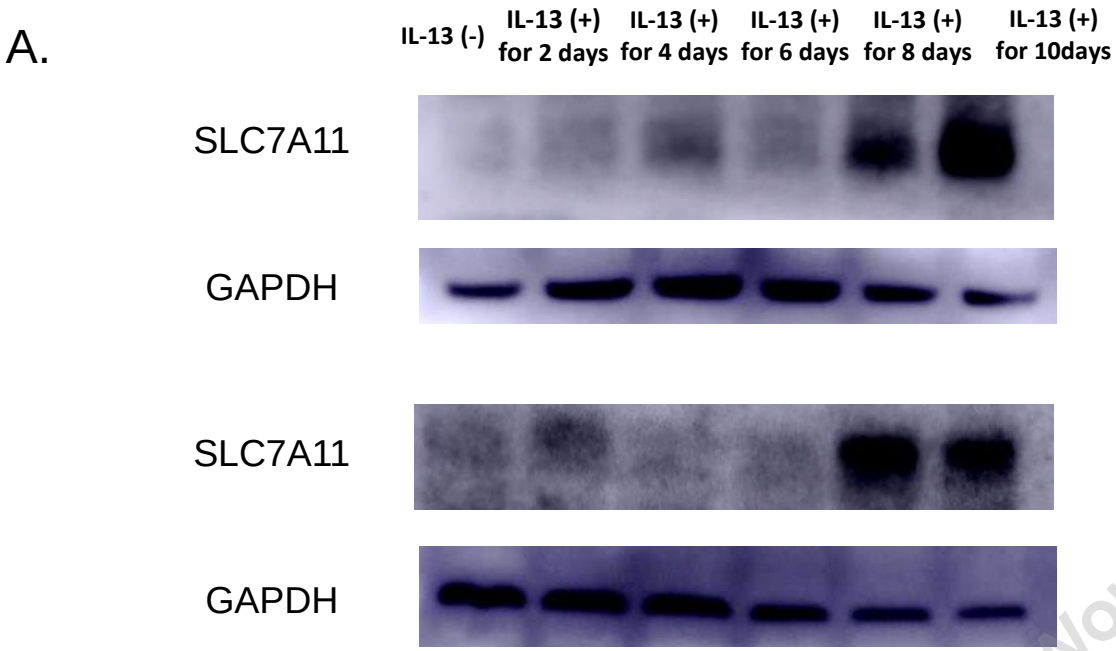

Fig. 2. (A) Representative western blots showing time course of SLC7A11 protein expression in response IL-13 stimulation *in vitro*. (**B**) Representative western bltos showing the inconsistent impact of ALOX15 siRNA knockdown on SLC7A11. (**C**) Densitometric analysis of the fold changes.

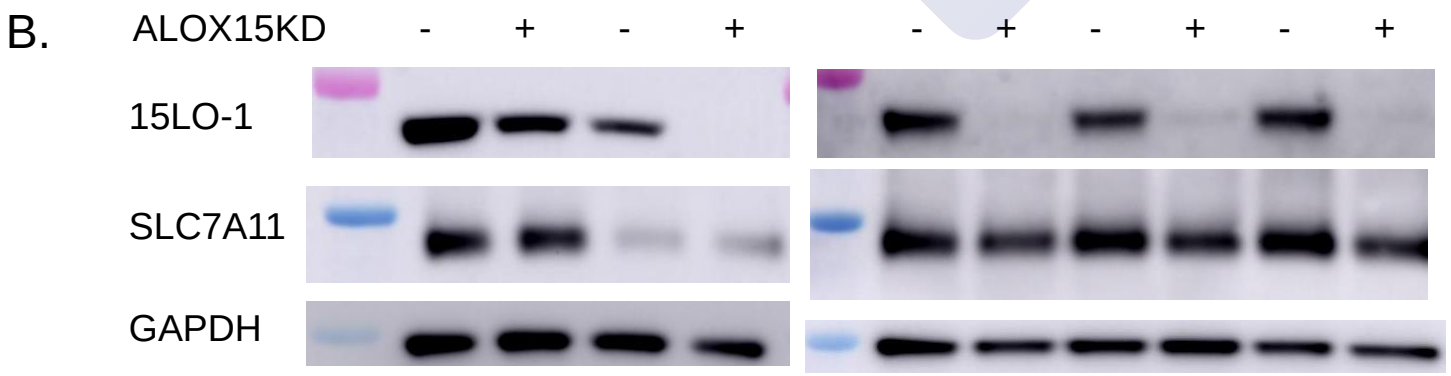

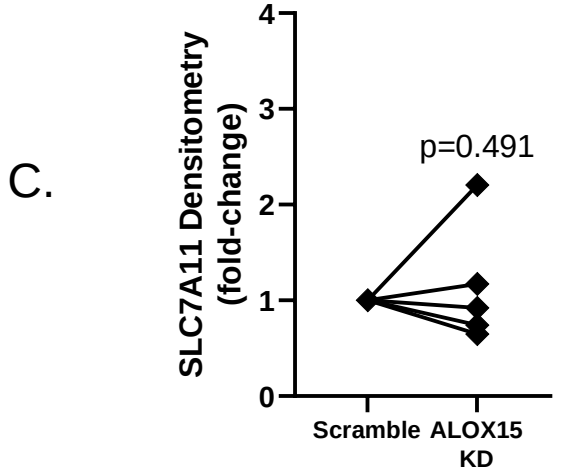

Supplemental Figure 3.

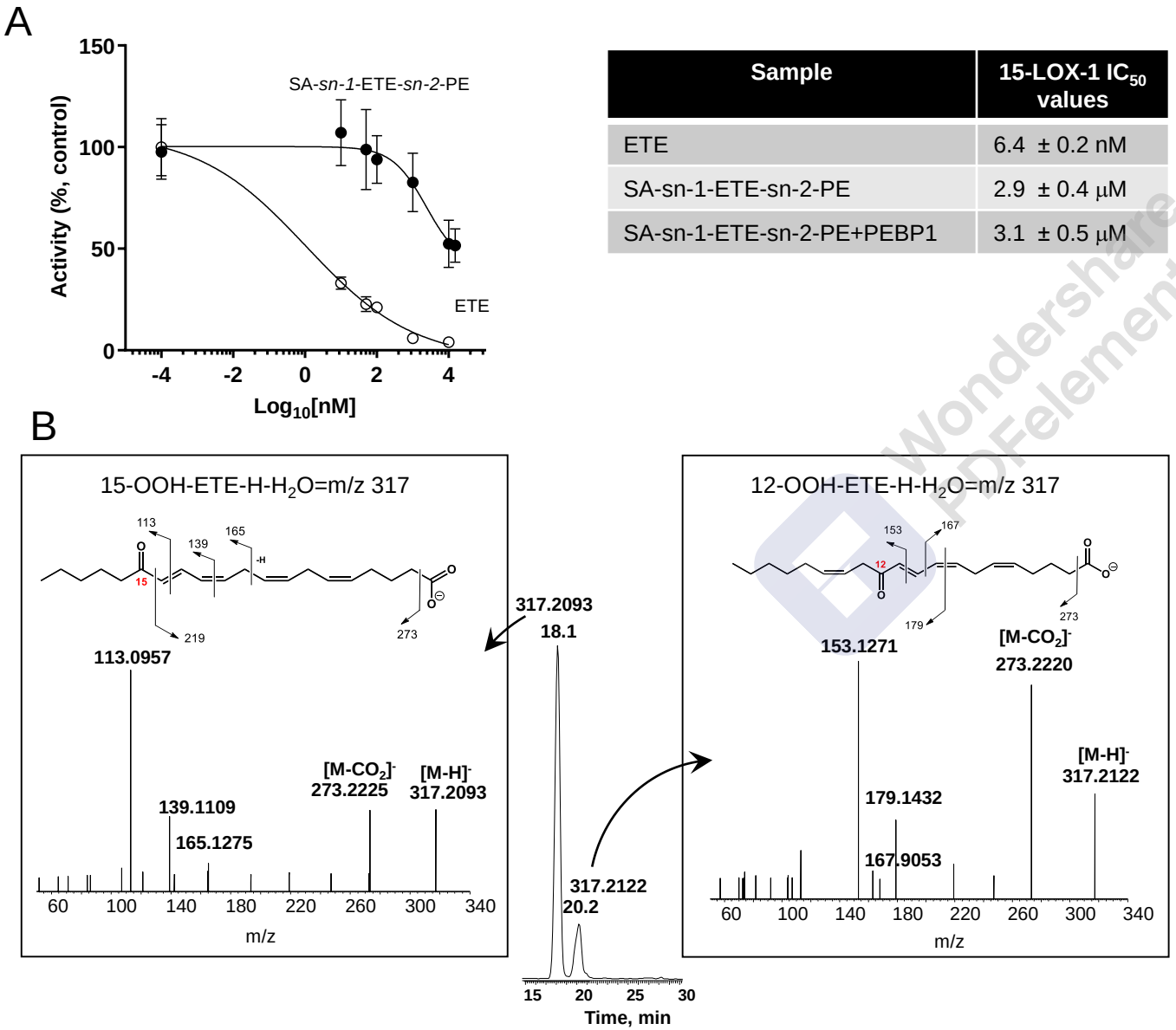

Sample	15-LOX-1 IC_{50} values
ETE	6.4 ± 0.2 nM
SA-sn-1-ETE-sn-2-PE	2.9 ± 0.4 μM
SA-sn-1-ETE-sn-2-PE+PEBP1	3.1 ± 0.5 μM

Fig 3. Effect of BLX2477 on oxidation of free eicosanotetraenoic acid (ETE) and stearoyl-sn-1-eicosatetraenoyl-sn-1-phosphatidylethanolamine (SA-sn-1-ETE-sn-2-PE) by 15-LOX-1 in the absence and in the presence of PEBP1.

(A) Concentration dependent inhibition of 15LO1 activity by BLX2477 in the presence of ETE (open circles) or in the presence of SA-sn-2-ETE-sn-2-PE (closed circles) (left panel). The data are presented as % of control. 100% of 15LO1 activity in the absence of BLX2477 was used as the control (n=5-7). IC_{50} values of 15LO1 for BLX2477. IC_{50} values were calculated using GraphPad Prism (GraphPad Software, Inc.)

(**B**) 15LO1 oxidation of ETE results in the formation of two oxidized products 15-OOH-ETE and 12-OOH-ETE. Base peak profile of oxygenated ETE formed during 15LO1-driven reaction (middle panel). MS^2 spectrum and structural formulas showing the fragments formed during the analysis of molecular ions with m/z 317.2 corresponding to 15-OOH-ETE without water (left panel) and 12-OOH-ETE without water (right panel).

Experimental conditions: ETE or SA-sn-1-ETE-sn-2-PE were integrated into OA-sn-1-OA-sn-2-PC (100 mM, at ratio of 1:1) liposomes and incubated with 15LO1 (0.4mM) for 2.5 and 5 min at 37ºC. Reaction was started by the addition of 3 μM 13 HpODE. At the end of incubation lipids were extracted and analyzed by LC/MS.

Supplemental Figure 4.

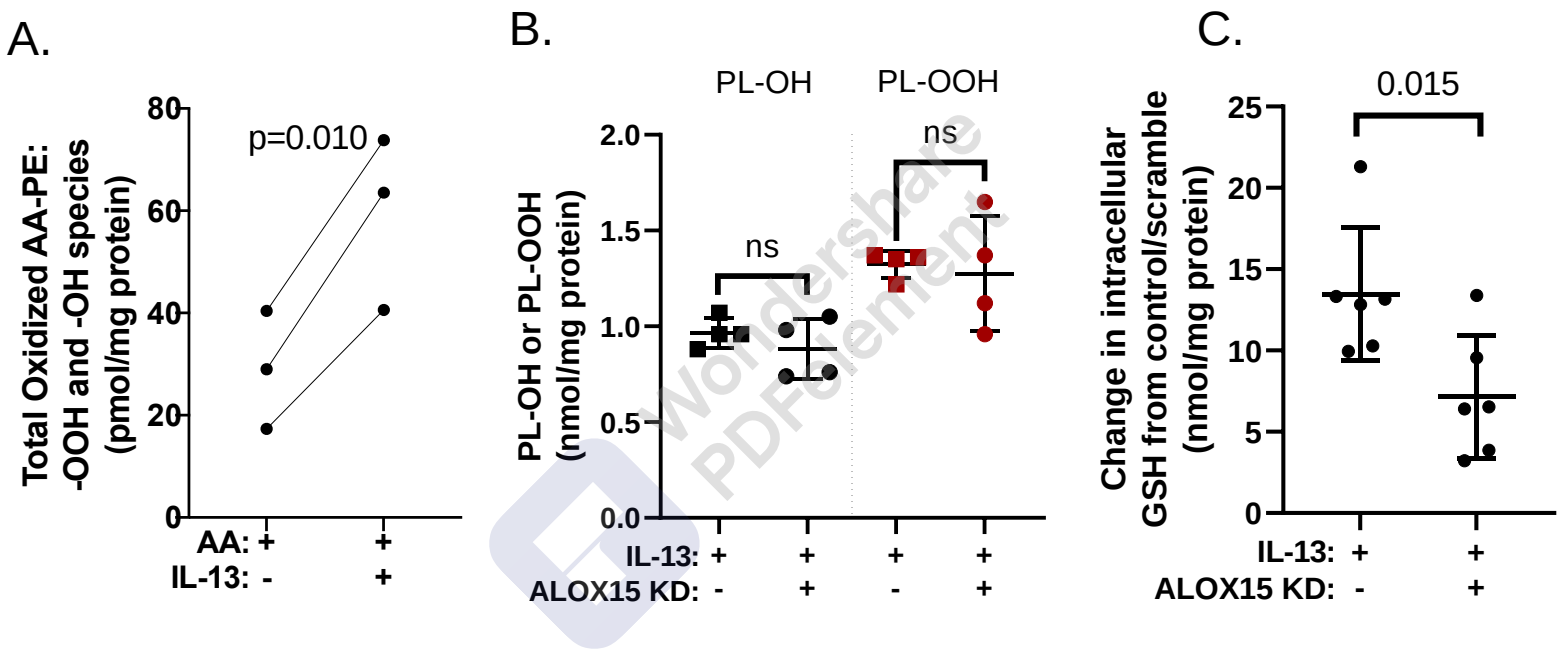

Fig 4. (A) Changes in hydroperoxy- and hydroxy-arachidonic acid (AA) species, including 15-HpETE and 15-HETE, following IL-13 with AA supplementation in HAECs. (**B**) Changes in total hydroperoxy- (PL-OOH) and hydroxy-phospholipids (PL-OH) following IL-13 and ALOX15/15LO1 KD compared to control/scramble in HAECs. (C) Changes in intracellular GSH.

Supplemental Figures.

Fig. 1. GSH and GSSG levels and GSH:GSSG measured by enzymatic method correlated strongly with high-performance liquid chromatography (HPLC) measurements (n=17).

Fig. 2. (A) Representative western blots showing time course of SLC7A11 protein expression in response IL-13 stimulation *in vitro*. (**B**) Representative western bltos showing the inconsistent impact of ALOX15 siRNA knockdown on SLC7A11. (**C**) Densitometric analysis of the fold changes.

Fig 3. Effect of BLX2477 on oxidation of free eicosanotetraenoic acid (ETE) and stearoyl-sn-1-eicosatetraenoyl-sn-1-phosphatidylethanolamine (SA-sn-1-ETE-sn-2-PE) by 15-LOX-1 in the absence and in the presence of PEBP1.

(A) Concentration dependent inhibition of 15LO1 activity by BLX2477 in the presence of ETE (open circles) or in the presence of SA-sn-2-ETE-sn-2-PE (closed circles) (left panel). The data are presented as % of control. 100% of 15LO1 activity in the absence of BLX2477 was used as the control (n=5-7). IC_{50} values of 15LO1 for BLX2477. IC_{50} values were calculated using GraphPad Prism (GraphPad Software, Inc.)

(**B**) 15LO1 oxidation of ETE results in the formation of two oxidized products 15-OOH-ETE and 12-OOH-ETE. Base peak profile of oxygenated ETE formed during 15LO1-driven reaction (middle panel). MS^2 spectrum and structural formulas showing the fragments formed

during the analysis of molecular ions with m/z 317.2 corresponding to 15-OOH-ETE without water (left panel) and 12-OOH-ETE without water (right panel).

Experimental conditions: ETE or SA-sn-1-ETE-sn-2-PE were integrated into OA-sn-1-OA-sn-2-PC(100 mM, at ratio of 1:1) liposomes and incubated with 15LO1 (0.4mM) for 2.5 and 5 min at 37°C. Reaction was started by the addition of 3 μM 13 HpODE. At the end of incubation lipids were extracted and analyzed by LC/MS.

Fig 4. (A) Changes in hydroperoxy- and hydroxy-arachidonic acid (AA) species, including 15-HpETE and 15-HETE, following IL-13 with AA supplementation in HAECs. (**B**) Changes in total hydroperoxy- (PL-OOH) and hydroxy-phospholipids (PL-OH) following IL-13 and ALOX15/15LO1 KD compared to control/scramble in HAECs. (**C**) Changes in intracellular GSH.

Supplemental Table 1. Characteristics of fresh epithelial cell subset

	HC (n = 11)	M/M (n = 4)	SA (n = 11)	P value
Age (years)	44 ± 14	35 ± 18	52 ± 11	0.189
Female/male	8/3	2/2	7/4	0.706
BMI (kg/m^2)	27 ± 4	28 ± 2	30 ± 7	0.478
History of exacerbation*, yes/no	NA	1/3	6/5	0.310
Inhaled corticosteroids, yes/no	NA	1/3	11/0	0.001
ACQ	NA	0.6 (0.2-1.2)	1.7 (1.3-3.0)	0.023
AQLQ	NA	6.3 (5.9-6.7)	5.2 (3.9-5.8)	0.013
FeNO (ppb)	11 (9-17)	31 (14-47)	37 (17-45)	0.011
FEV$_1$ (% predicted)	102 ± 13	98 ± 17	65 ± 25	<0.001

Data as means ± SDs

34 p values by ANOVA, Mann-Whitney, Kruskal-Wallis, or χ^2 tests

35 Exacerbation*, self-reported use of systemic corticosteroid ≥3 days in past 12 months

Supplemental Table 2. Relationships between extracellular (BAL fluid) and intracellular GSH pathways in asthma and HCs

	BAL fluid		
	GSH (μM)	GSSG (μM)	GSH:GSSG
Intracellular			
GSH (nmol/mg protein)	**r=0.41** **p=0.037**	r=-0.29 p=0.156	**r=0.58** **p=0.002**
GSSG (nmol/mg protein)	r=0.26 p=0.191	r=-0.09 p = 0.645	r=0.33 p=0.104
GSH:GSSG	r=0.13 p=0.517	r= -0.19 p= 0.352	r=0.24 p=0.234

Supplemental Table 3. Non-parametric correlations for BAL eosinophils (absolute, % BAL cells) and GSH, GSSG and GSH:GSSG

Eosinophils

	Absolute eosinophil numbers	% BAL Cells
BAL Fluid:		
GSH	rho=0.02	rho=-0.08
	p=0.877	p=0.417
GSSG	rho=-0.01	rho=0.05
	p=0.938	p=0.644
GSH:GSSG	rho=-0.05	rho=-0.18
	p=0.610	p=0.078
Intra-epithelial:		
GSH	rho=-0.25	rho=-0.33
	p=0.227	p=0.102
GSSG	rho=-0.26	rho=-0.29
	p=0.199	p=0.148

GSH:GSSG	rho=-0.07	rho=-0.14
	p=0.730	p=0.482

Supplemental Table 4. Non-parametric corrleations of inflammatory cells (% BAL cells) versus BAL fluid and intracellular/intra-epithelial GSH, GSSG, and GSH:GSSG.

Other Inflammatory Cells

	Neutrophils (% BAL cells)	**Macrophages (% BAL cells)**	**Lymphocytes (% BAL cells)**
BAL Fluid:			
GSH	rho=-0.06	rho=0.01	rho=-0.01
	p=0.586	p=0.989	p=0.914
GSSG	rho=0.16	rho=-0.15	rho=0.07
	p=0.147	p=0.156	p=0.542
GSH:GSSG	rho=-0.19	rho=0.14	rho=-0.09
	p=0.089	p=0.206	p=0.431

Intra-epithelial:			
GSH	rho=-0.07	rho=0.01	rho=0.13
	p=0.725	p=0.985	p=0.527
GSSG	rho=0.15	rho=0.17	rho=-0.12
	p=0.481	p=0.403	p=0.557
GSH:GSSG	rho=-0.32	rho=0.01	rho=0.07
	p=0.117	p=0.956	p=0.744

62

63

Supplemental Table 5. Correlation of T2 signature genes and ALOX15 expression.

	ALOX15 expression
CCL26 expression	**r=0.58**
	p<0.001
MUC5AC expression	**r=0.41**
	p<0.001
NOS2 expression	**r=0.67**
	p<0.001
POSTN expression	**r=0.56**
	p<0.001

Bold p-values pass Bonferonni Correction